Available online at www.sciencedirect.com

ScienceDirect

Procedia IUTAM 19 (2016) 219 – 227

Procedia IUTAM

www.elsevier.com/locate/procedia

IUTAM Symposium Analytical Methods in Nonlinear Dynamics

Discontinuity Induced Bifurcations in Nonlinear Systems

B. Santhosh, S. Narayanan, C. Padmanabhan

Department of Mechanical Engineering, Indian Institute of Technology Madras, Chennai, India, 600036

Abstract

Nonlinear systems involving impact, friction, free-play, switching etc. are discontinuous and exhibit sliding and grazing bifurcations when periodic trajectories interact with the discontinuity surface which are classified into crossing sliding, grazing sliding, adding sliding and switching sliding bifurcations depending on the nature of the bifurcating solutions from the sliding surface. The sudden onset of chaos and the stick-slip motion can be explained in terms of these bifurcations. This paper presents numerical and numerical-analytical methods of studying the dynamics of harmonically excited systems with discontinuous nonlinearities representing them as Filippov systems. The switch model based numerical integration schemes in combination with the time domain shooting method are adopted to obtain the periodic solutions and the bifurcations.

Peer-review under responsibility of organizing committee of IUTAM Symposium Analytical Methods in Nonlinear Dynamics

Keywords: Filippov systems; Discontinuity Induced Bifurcations; Switch Model; SD oscillator; Dry Friction

1. Introduction

Nonlinear dynamical systems can have either continuous or discontinuous nonlinearities or both. Rotor-stator rub interactions in gas turbines, dry friction damping in turbomachinery bladed systems, complex frictional contact and backlash in gear teeth and intermittent separation and contact of tool and work piece in metal cutting are examples for systems with discontinuous nonlinearities. In electrical systems the switching electrical circuits represent discontinuous system. The equation of motion suddenly changes depending on the transition of a particular state of the system crossing a barrier. Accurate modeling and efficient analysis framework are necessary to capture the times of these transitions and switch from one set of equations to another set of equations and apply the conditions to obtain the dynamics. The discontinuous functions in the equations of motion can be approximated by smooth functions and the study on the dynamics of the approximated smooth system can identify classical bifurcations but fail to identify the discontinuity induced bifurcations (DIB). Nonlinear systems with discontinuous nonlinearities can be modeled as Filippov systems[1] which allows the use of event driven numerical integration and shooting method based on a switch model representation to integrate the equations of motion and identify the DIB[2].

* Santhosh B.
E-mail address: santhoshbpillai@gmail.com

Peer-review under responsibility of organizing committee of IUTAM Symposium Analytical Methods in Nonlinear Dynamics
doi:10.1016/j.piutam.2016.03.028

In this paper, the dynamics of two harmonically excited single degree of freedom (sdf) discontinuous oscillators are investigated to identify the DIB. The smooth and discontinuous (SD) oscillator in the discontinuous phase shows a sudden transition from a period 1 solution to chaotic solution through a grazing bifurcation. The sdf nonlinear system with damping and stiffness nonlinearities on a moving belt with Coulomb friction between the mass and the belt show adding sliding, switching sliding and crossing sliding bifurcations apart from the grazing bifurcation. The procedure to investigate the dynamics of a two-dimensional Filippov system is also outlined.

2. Filippov Systems

In the Filippov representation illustrated in Fig. 1, S_1 and S_2 be the two regions in the phase space where the associated vector fields F_1 and F_2 are smooth and Σ be the discontinuous surface separating S_1 and S_2. The vector field along Σ can be represented as a convex combination of the two smooth vector fields F_1 and F_2 as

$$\overline{co}(F_1(x), F_2(x)) = \{f_F : x \in \mathbb{R}^n \to \mathbb{R}^n : f_F = (1-\alpha_1)F_1 + \alpha_1 F_2, \alpha_1 \in [0,1]\} \tag{1}$$

The discontinuity surface Σ is represented by a scalar function $H(x)$ with a non-vanishing gradient. Therefore $S_1 = \{x \in \mathbb{R}^2 : H(x) > 0\}$, $S_2 = \{x \in \mathbb{R}^2 : H(x) < 0\}$ and $\Sigma = \{x \in \mathbb{R}^2 : H(x) = 0\}$.

Other than the Filippov convex method, Utkins equivalent control method can also be used to represent the vector field along the sliding surface as[3]

$$F_{ij}(x) = \frac{F_1 + F_2}{2} + \mu_{ij}\frac{F_2 - F_1}{2} \tag{2}$$

where $-1 < \mu_{ij}(x) < 1$. The expression for $\mu_{ij}(x)$ can be obtained in terms of F_1 and F_2 as

$$\mu_{ij}(x) = -\frac{\langle \nabla H, F_1\rangle + \langle \nabla H, F_2\rangle}{\langle \nabla H, F_2\rangle - \langle \nabla H, F_1\rangle} \tag{3}$$

where $\nabla H = \frac{\partial H}{\partial \mathbf{x}}$ and $\langle a, b\rangle$ is the inner product. The state of the system can initially be in one of the smooth regions. Let the solution be initially at region S_1 for which $H(x) > 0$. As time unwinds, it may approach Σ and there exist two possibilities, (i) the solution leaves Σ and enters S_2 (transversal intersection) or (ii) it remains on Σ (sliding). These are shown in Fig. 1.

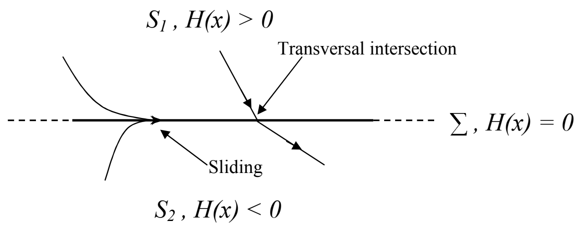

Fig. 1. Filippov representation.

3. Discontinuity induced bifurcations

Apart from classical bifurcations, discontinuous systems exhibit another class of bifurcations known as the discontinuity induced bifurcations (DIB) when a periodic trajectory interacts with the boundary of the discontinuity surface. Filippov systems are a class of systems which exhibit DIB. Four different types of co-dimension one bifurcations are observed in Filippov systems. They are (i) crossing sliding (ii) grazing sliding (iii) switching sliding and (iv) adding sliding bifurcations[4]. In crossing sliding bifurcation, the trajectory crosses the switching manifold transversely precisely at the boundary of the sliding strip as shown in Fig. 2(a). In grazing sliding bifurcation, which is shown in Fig. 2(b), the trajectory which is initially lying in one of the subspaces grazes the sliding surface with the variation of the parameter. Occasionally, the grazing bifurcation leads to the sudden onset of chaos from a periodic solution. In switching sliding bifurcation shown in Fig. 2(c), the trajectory which is initially confined to one of the subspace and the sliding region, intersects the boundary of the sliding surface and passes to the other subspace and then back to the sliding surface. In adding sliding bifurcation, with the parameter variation, additional slipping segments are produced along the sliding segment.

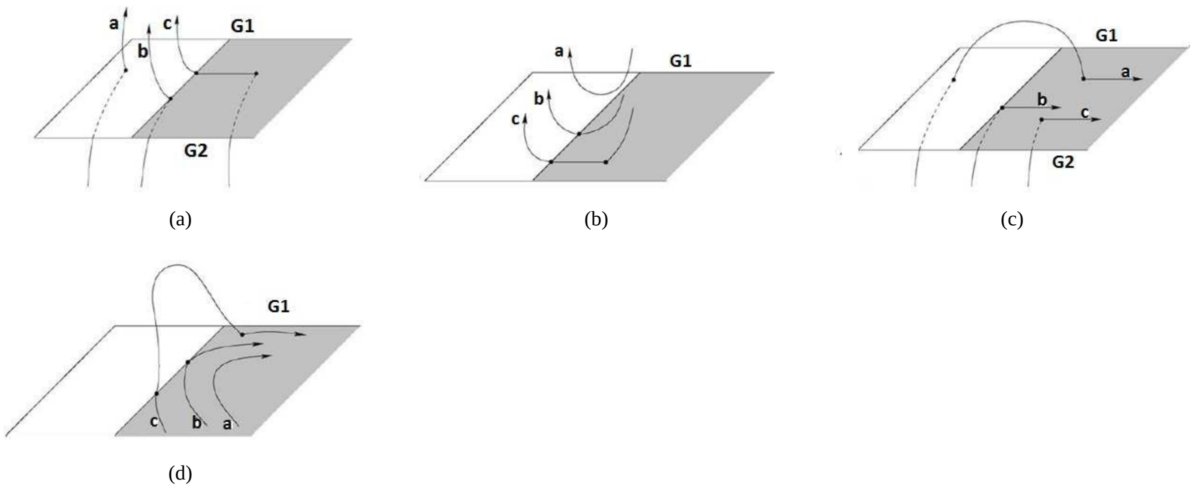

Fig. 2. Sliding bifurcations in Filippov systems (a) Crossing sliding bifurcation (b) Grazing sliding bifurcation (c) Switching sliding bifurcation and (d) Adding sliding bifurcation[4].

The following general conditions must be satisfied for all the four cases of sliding bifurcations at the bifurcation point $(\mathbf{x}^*, t^*)$[4].

$$H(\mathbf{x}^*) = 0; \quad \nabla H(\mathbf{x}^*) \neq 0; \quad \langle \nabla H, F_1 \rangle |_{(\mathbf{x}^*,t^*)} = 0 \tag{4}$$

Other conditions for specific bifurcations are the following

(a) crossing sliding and grazing sliding

$$\left\langle \nabla H, \frac{\partial F_1}{\partial \mathbf{x}} F_1 \right\rangle |_{(\mathbf{x}^*,t^*)} > 0 \tag{5}$$

(b) switching sliding

$$\left\langle \nabla H, \frac{\partial F_1}{\partial \mathbf{x}} F_1 \right\rangle |_{(\mathbf{x}^*,t^*)} < 0 \tag{6}$$

(c) adding sliding

$$\left\langle \nabla H, \left(\frac{\partial F_1}{\partial \mathbf{x}} \right)^2 F_1 \right\rangle |_{(\mathbf{x}^*,t^*)} < 0 \tag{7}$$

4. Examples

In this section, the DIB exhibited by two discontinuous nonlinear oscillators are explained. The first example is the harmonically excited sdf smooth and discontinuous (SD) oscillator and the second example is a harmonically excited sdf oscillator with nonlinear damping and stiffness with the mass moving on a sliding belt with Coulomb friction between the mass and the belt.

4.1. Smooth and Discontinuous (SD) Oscillator

The SD oscillator is representative of a snap-through truss system and its schematic model is shown in Fig. 3 Assuming the damping in the system to be of viscous type, the non-dimensional equations of motion of the oscillator

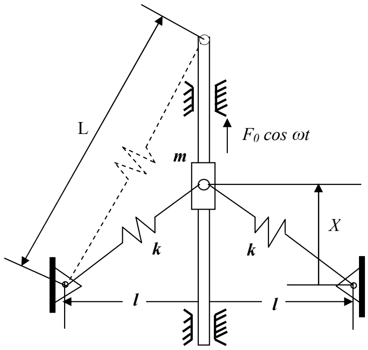

Fig. 3. The smooth and discontinuous oscillator

can be expressed as[5]

$$x'' + 2\zeta x' + x\left(1 - \frac{1}{\sqrt{x^2 + \alpha^2}}\right) = f_0 \cos(\Omega\tau) \tag{8}$$

The parameter α is known as the smoothness parameter. When $\alpha > 0$, the nonlinearity associated with the system is continuous and for $\alpha = 0$, the system nonlinearity is discontinuous. The dynamics of the SD oscillator has been investigated both in the time and frequency domains[5]. The equation of motion of the SD oscillator for the discontinuous case is given by

$$x'' + 2\zeta x' + (x - sgn(x)) = f_0 \cos(\Omega\tau) \tag{9}$$

where $sgn(x)$ is the *signum* function which makes the system discontinuous. Filippov representation for the discontinuous SD oscillator is given by

$$F_1(\mathbf{x}) = \begin{pmatrix} x_2 \\ f_0 \cos(\Omega\tau) - 2\zeta x_2 - x_1 + 1 \end{pmatrix} \qquad \text{if} \quad x_1 \in S_1 \tag{10}$$

$$F_2(\mathbf{x}) = \begin{pmatrix} x_2 \\ f_0 \cos(\Omega\tau) - 2\zeta x_2 - x_1 - 1 \end{pmatrix} \qquad \text{if} \quad x_1 \in S_2 \tag{11}$$

The discontinuity surface Σ between the two smooth surfaces is represented by a scalar function $H(x) = x_1 = 0$. The normal to the discontinuity surface is given by $[1 \quad 0]^T$.

The equation of motion is numerically integrated using the event based integration with $f_0 = 0.25, \zeta = 0.0141$. The bifurcation diagram obtained with Ω as the parameter is shown in Fig. 4. When Ω is increased from a lower value, the discontinuous oscillator has a large amplitude period 1 (P1) motion which suddenly bifurcates to a chaotic solution at $\Omega = 0.8667$. At $\Omega = 1.145$, the chaotic solution suddenly changes to a P1 solution. Apart from the chaotic solutions, narrow windows of higher order periodic solutions are also observed. The period 1 (P1) solutions obtained by harmonic balance method (HBM) are represented in the bifurcation diagram by the symbol '○'.

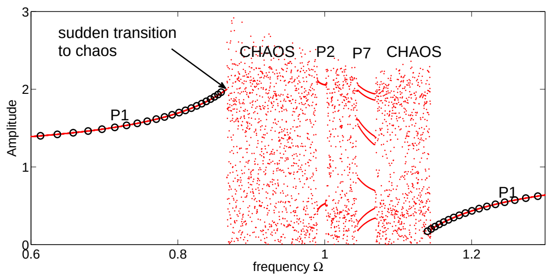

Fig. 4. Bifurcation diagram with Ω as the parameter. P_1- period 1 solution, ○- P_1 solution obtained by HBM

The Lyapunov spectrum obtained with Ω as the parameter is shown in Fig. 5. The Lyapunov exponents are computed using the method proposed by Wolf et al.[6] and approximating the *signum* function by an arc tangent function[7,8]. The Lyapunov exponent also shows a sudden jump at $\Omega = 0.8667$ to a positive value confirming chaos

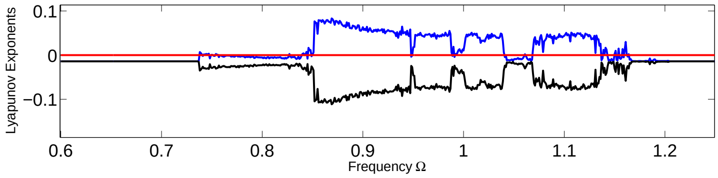

Fig. 5. Lyapunov spectrum with Ω as the parameter

in the system. The sudden transition of the periodic solution to chaotic solution in the bifurcation diagram can be explained in the context of DIB. The time histories and phase plane plot of the P1 solution for $\Omega = 0.7$ are shown in Figs. 6(a) and (b). The periodic solution is confined to one of the smooth region S_1 where $H(x) > 0$. The discontinuity

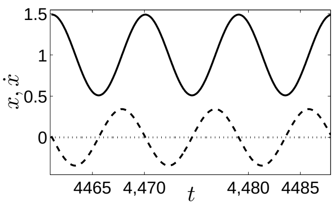

(a)

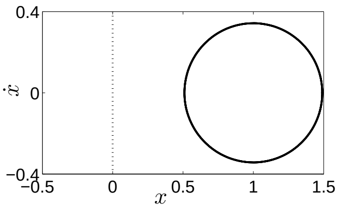

(b)

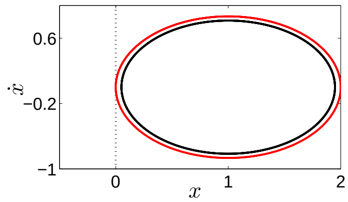

(c)

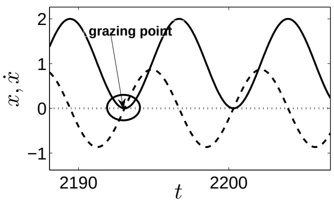

(d)

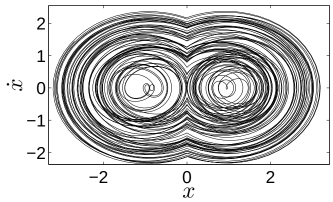

(e)

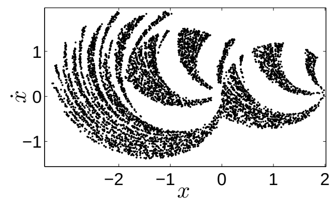

(f)

Fig. 6. (a)-(b) Time history and phase plane plot for $\Omega = 0.7$ (c)-(d) Grazing of the periodic orbit with the discontinuity surface (e)-(f) chaotic attractor for $\Omega = 0.87$

surface is shown by the straight dotted line in the time histories and phase plane plots. When the parameter Ω is varied, the amplitude of the motion grows and when $\Omega = 0.86672$, the periodic orbit grazes the discontinuity surface tangentially. This condition is shown in Fig. 6(c). The phase plane plot shows the periodic orbit just before grazing (black) and the periodic orbit at the time of grazing (red). From the time histories in Fig. 6(d) it is observed that the displacement and velocity both are zero at the time of grazing. The sudden onset of chaos beyond the bifurcation value $\Omega = 0.86667$ is thus due to the grazing bifurcation which is a DIB. The phase plane plot and the strange attractor for $\Omega = 0.87$ are shown in Figs. 6(e) and (f).

4.2. *Dynamics of system with friction*

In this section, the dynamics of a harmonically excited sdf friction oscillator shown in Fig. 7 is investigated to identify the DIB.

Similar systems have been investigated by Awrejcewicz et al.[9,10] to understand the stick-slip dynamics and chaos. The equation of motion for the above system can be expressed as

$$m\ddot{x} - c_1(\dot{x} - v) + c_2(\dot{x} - v)^3 + k_1 x + k_2 x^3 + \mu mg\ sgn(\dot{x} - v) = F_0 \cos(\omega t) \tag{12}$$

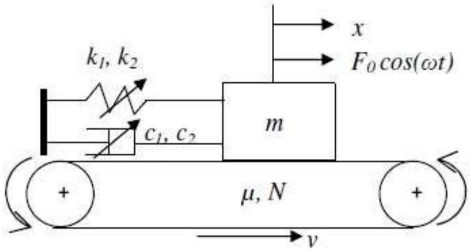

Fig. 7. Mass on a moving belt with additional nonlinearities

If $|\dot{x} - v| < \epsilon$ and $|k_1 x + k_2 x^3 - F_0 \cos(\omega t)| < \mu mg$, then the mass sticks to the belt and is carried along with the belt. When the relative velocity is large and when the restoring force is able to overcome the frictional force, then the mass starts slipping over the belt and complex motions arise in different parameter regimes. Eq. (12) can be expressed as

$$\ddot{x} - \alpha g(\dot{x} - v) + \beta g(\dot{x} - v)^3 + \gamma_1 x + \gamma_2 x^3 + \mu g \ sgn(\dot{x} - v) = f_0 \cos(\omega t) \tag{13}$$

where $\alpha = \frac{c_1}{mg}, \beta = \frac{c_2}{mg}, \gamma_1 = \frac{k_1}{m}, \gamma_2 = \frac{k_2}{m}$ and $f_0 = \frac{F_0}{m}$. The system can be represented as a Filippov system as given below

$$F_1(x) = \begin{cases} x_2 \\ f_0 \cos(\omega t) + \alpha g(x_2 - v) - \beta g(x_2 - v)^3 - \gamma_1 x_1 - \gamma_2 x_1^3 - \mu g, & H(x) > 0 \end{cases} \tag{14}$$

$$F_2(x) = \begin{cases} x_2 \\ f_0 \cos(\omega t) + \alpha g(x_2 - v) - \beta g(x_2 - v)^3 - \gamma_1 x_1 - \gamma_2 x_1^3 + \mu g, & H(x) < 0 \end{cases} \tag{15}$$

where $x_1 = x$ and $x_2 = \dot{x}$. The scalar function $H(x) = x_2 - v$ corresponds to the discontinuity surface.

The dynamics of the system is studied with the following parameters. $f_0 = 10$ m/s^2, $g = 9.81$ m/s^2, $\mu = 0.6$, $\alpha = -0.05$ s/m, $\beta = 0$, $\gamma_1 = 10$ s$^-2$, $\gamma_2 = 0$ and $v = 1$ m/s. The system is considered as a Filippov system and integrated numerically employing the switch model[2]. The variation of the maximum value of the velocity $\dot{x}_{max}$ of the mass as a function of ω is shown in Fig. 8.

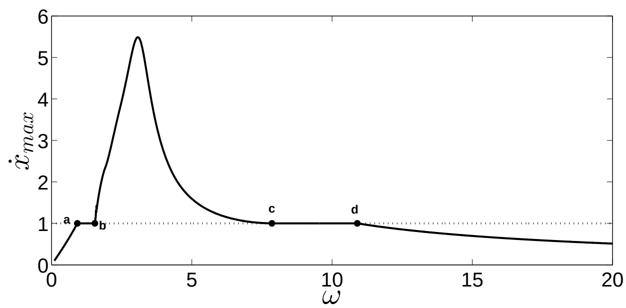

Fig. 8. Frequency response.

The excitation frequency ω is varied in the range 0-20. The dotted line shown in the figure corresponds to $\dot{x} - v = 0$, the discontinuity surface. Once the solution undergoes sliding (sticking of the mass), the response remains in the sliding region for a finite duration of time period. For the two regions **a-b** and **c-d**, a part of the trajectory undergoes sliding and the other part is confined to one of the smooth regions (the mass is slipping). To explain the different dynamic phenomena associated with this system, the phase plane plots of the response for different ω values along the frequency response curve in Fig. 8 are obtained by the shooting method and are shown in Fig. 9. When $\omega = 0.92$ which is marked by the point **a** in Fig. 8 the solution just grazes the discontinuity surface as shown in Fig.9(a). With increase of ω a part of the trajectory remains in the sliding surface as observed in Fig. 9(b). When $\omega = 1.55$, marked

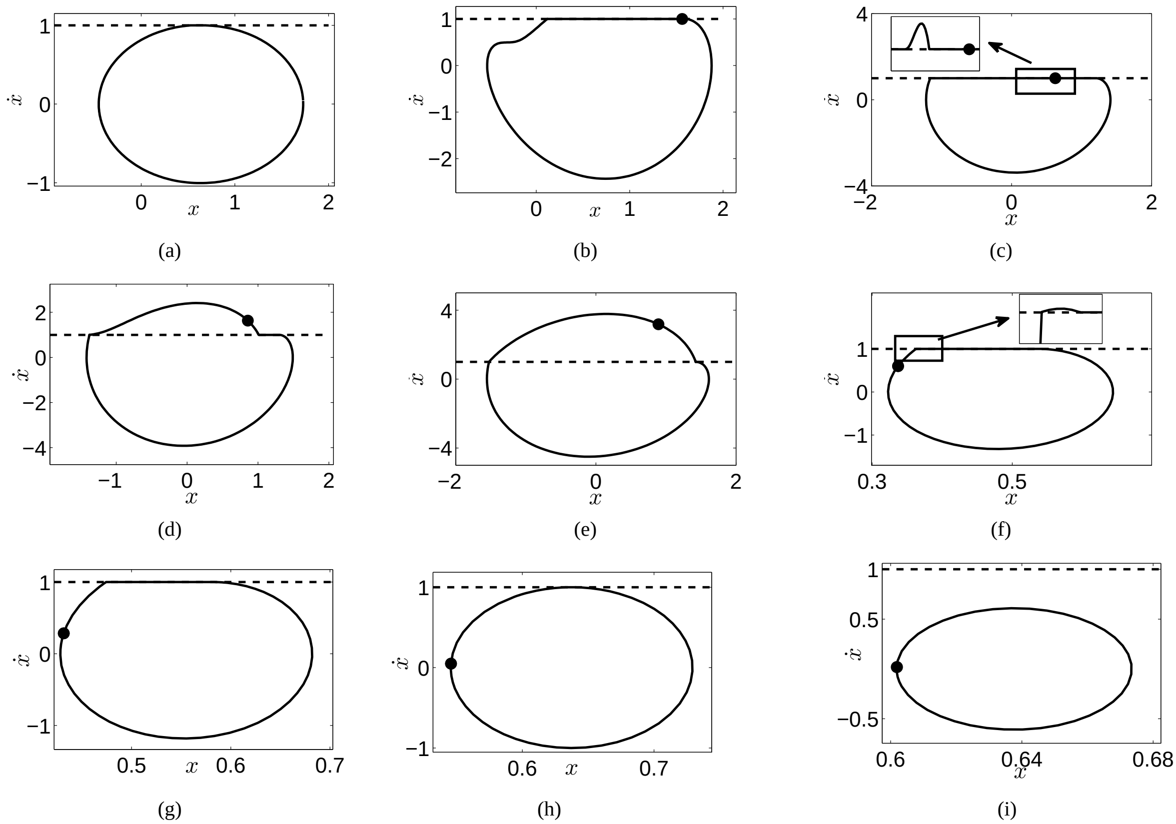

Fig. 9. Phase plane plots (a) $\omega = 0.92$ [**a**] (b) $\omega = 1.3$ (c) $\omega = 1.55$ [**b**] (d) $\omega = 1.95$ (e) $\omega = 2.44$ (f) $\omega = 7.85$ [**c**] (g) $\omega = 9.1$, (h) $\omega = 10.9$ [**d**] (i) $\omega = 17$.(Letters in square brackets corresponds to the points marked in Fig. 8). • - Poincaré points.

by the point **b** in Fig. 8, a segment of trajectory crosses the sliding region and joins back the sliding surface. This is the case of adding sliding bifurcation which is a DIB. This region is marked in Fig. 9(c) within a rectangle. The zoomed view of the same is also shown in the figure. With further increase of ω, this slipping segment grows in size and it touches the boundary on the left side and the sliding segment is limited just to the right of the phase plane. This behavior is shown in Fig. 9(d) for $\omega = 1.95$. With further increase in ω, the sliding region on the right of the phase plane also disappears and the solution after reaching the sliding surface from one of the subspace does not remain on the sliding surface but moves to the other subspace. This case of transversal intersection is shown in Fig. 9(e).

If the frequency is decreased from a larger value of $\omega = 20$, the solution initially remains in the subspace $\dot{x} - v < 0$ which is shown in Fig. 9(i) for $\omega = 17$. With further decrease in the value of ω, the solution grazes the discontinuity surface when $\omega = 10.9$ which is marked by the point **d** in Fig. 8. A sliding segment of the trajectory is thus formed with further decrease in ω. The phase plane plot shown in Fig. 9(g) for $\omega = 9.1$ shows that the solution remains in one of the subspace and in the sliding region. When $\omega = 7.85$, marked by the point **c** in Fig. 8 the sliding segment shows the generation of an additional slipping segment at the boundary. This region is marked with a rectangle and the zoomed view of the same is shown in Fig. 9(f). This case is known as a switching sliding bifurcation which is classified under the DIB.

The dynamics of the above system is further investigated for the following parameters $f_0 = 10$ m/s^2, $g = 9.81$ m/s^2, $\mu = 0.6, \alpha = -0.05$ s/m, $\beta = 0$, $\gamma_1 = 0$, $\gamma_2 = 10000$ m/s^2 and $v = 1$ m/s. The bifurcation diagram is also obtained for the range $4.2 \leq \omega \leq 4.7$ and is shown in Fig. 10.

The bifurcation diagram shows a P1 solution suddenly bifurcating into a chaotic solution. This transition takes place at $\omega = 4.565$. The phase plane plot of the P1 solution for $\omega = 4.56$ is shown in Fig. 11 (a). The solution is bound to the subspace $\dot{x} < v$. With slight increase in the value of ω, the P1 solution grazes the discontinuity

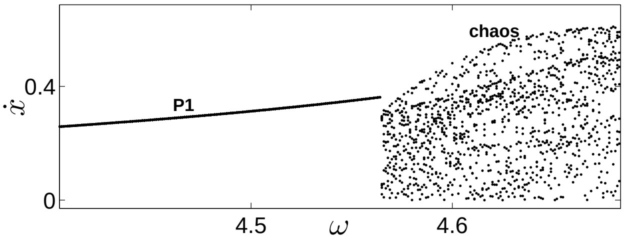

Fig. 10. Bifurcation diagram with ω as the parameter for $4.2 \leq \omega \leq 4.7$.

surface. With further increase in the value of ω, the solution starts sliding over the discontinuity surface. The grazing phenomenon can lead to a sudden onset of chaos. The phase plane plot of the chaotic solution for $\omega = 4.565$ along with the Poincaré section is shown in Fig. 11(b).

This sudden transition of the periodic solution to chaotic solution when the periodic solution just reaches the discontinuity surface is due to the grazing sliding bifurcation which is again a DIB. Similar behavior of grazing bifurcation without sliding was observed for the case of the smooth and discontinuous (SD) oscillator. The largest Lyapunov exponent obtained as a function of frequency ω is shown in Fig. 11(c). It is observed that at $\omega = 4.565$, the Lyapunov exponent jumps to positive value which confirms chaos in the system.

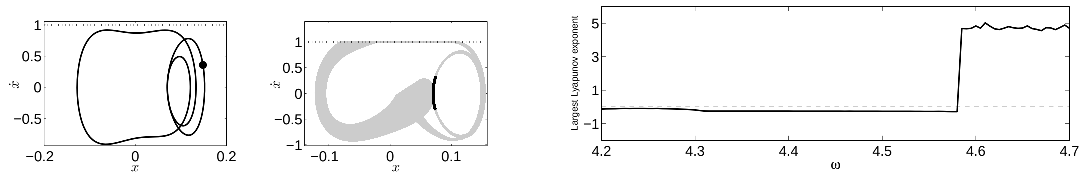

(a) (b) (c)

Fig. 11. Sudden transition to chaos (a) P1 solution for $\omega = 4.56$ (b) chaotic solution for $\omega = 4.565$.

5. Estimation of Lyapunov exponent based on chaos synchronization

The method of chaos synchronization can be used to estimate the largest Lyapunov exponent of non-smooth systems [11]. For this purpose, the equations of motion along with an augmented set of equations are integrated numerically till synchronization takes place between the two systems. For the sdf system shown in Fig.7, the equations of motions along with the augmented system can be represented as given below.

$$\begin{aligned}
\dot{x}_1 &= x_2 \\
\dot{x}_2 &= f_0 \cos(\omega t) + \alpha g(x_2 - v) - \beta g(x_2 - v)^3 - \gamma_1 x_1 - \gamma_2 x_1^3 - \mu g\ sgn(x_2 - v) \\
\dot{x}_3 &= x_4 + \epsilon(x_1 - x_3) \\
\dot{x}_4 &= f_0 \cos(\omega t) + \alpha g(x_2 - v) - \beta g(x_2 - v)^3 - \gamma_1 x_1 - \gamma_2 x_1^3 - \mu g\ sgn(x_2 - v) + \epsilon(x_2 - x_4)
\end{aligned} \tag{16}$$

In Filippov representation, the above system becomes a two dimensional one with discontinuity surfaces $\Sigma_2 : H_2(x) = x_2 - v = 0$ and $\Sigma_4 : H_4(x) = x_4 - v = 0$. The switch model representation of the same is shown in Fig.12(a) with $F_1$to F_4 as the smooth surfaces and $\Sigma = \Sigma_2 \cap \Sigma_4$ the intersection of the two discontinuous surfaces. Apart from the conditions for sliding along Σ_2 and Σ_4, the conditions for sliding along Σ are

$$\begin{aligned}
&n_1^T F_4 < 0, n_1^T F_2 > 0, n_2^T F_4 < 0, n_2^T F_3 > 0 \\
&n_1^T F_4 < 0, n_1^T F_2 < 0, n_2^T F_4 < 0, n_2^T F_3 < 0
\end{aligned} \tag{17}$$

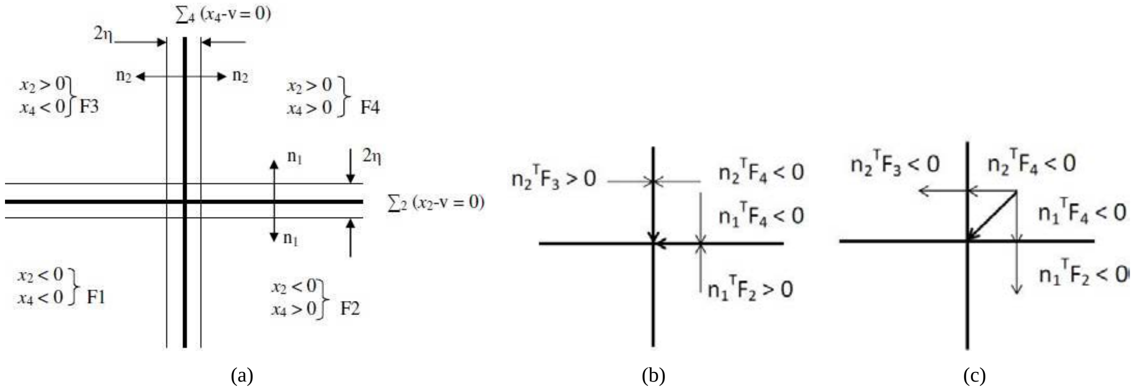

Fig. 12. (a) Switch model representation of two dimensional Filippov system (b)-(c) Attractive sliding modes

These conditions are shown in Figs.12 (b)-(c) assuming attractive sliding mode along Σ. The vector field along Σ can be expressed as

$$F(\Sigma) = \lambda_1 F_1 + \lambda_2 F_2 + \lambda_3 F_3 + \lambda_4 F_4 \tag{18}$$

with $\sum_i \lambda_i = 1$. The equations of motion (12) can be integrated numerically using the switch model and the lowest value of ϵ for which the synchronization takes place can be estimated as the largest Lyapunov exponent.

6. Conclusions

In this paper, the discontinuity induced bifurcations observed in the smooth and discontinuous (SD) oscillator and in systems with friction are investigated. The modeling of these systems as Filippov systems enabled the identification of these bifurcations. In SD oscillator, the sudden transition of the periodic solution to chaotic solution happens through the grazing bifurcation which is a DIB. In systems with friction, the stick-slip phenomenon is explained with the help of the sliding bifurcations such as the adding sliding, switching sliding and crossing sliding bifurcations. A method based on the switch model representation to analyze two dimensional Filippov system is also outlined.

References

1. Filippov AF. Differential equations with discontinuous right hand side. *American Mathematical Society Transl.* 1964;**42**:199-231.
2. Leine RI, Nijmeijer H. Dynamics and bifurcations of non-smooth mechanical systems. *Springer Science and Business* 2013;**18**.
3. Utkin VI. Sliding modes in control and optimization. *Springer* 1992;**116**
4. Di Bernardo M, Kowalczyk P, Nordmark A. Sliding bifurcations: a novel mechanism for the sudden onset of chaos in dry friction oscillators. *Int.Journal of Bifurcation and Chaos* 2003;**13(10)**: 2935-2948
5. Santhosh B, Narayanan S, Padmanabhan C. Numeric-analytic solutions of the smooth and discontinuous oscillator. *Int.Journal of Mechanical Sciences* 2014;**84**: 102-119.
6. Wolf A, Swift JB, Swinney HL, Vastano JA. Determining Lyapunov exponents from a time series.*Physica D: Nonlinear Phenomena* 1985;**16(3)**: 285-317.
7. Narayanan S, Jayaraman K. Chaotic vibration in a non-linear oscillator with Coulomb damping.*Journal of Sound and Vibration* 1991;**146(1)**: 17-31.
8. Awrejcewicz J, Feckan M, Olejnik P . On continuous approximation of discontinuous systems.*Nonlinear Analysis Theory, Methods and Applications* 2005;**62(7)**: 1317-1331.
9. Awrejcewicz J, Olejnik P . Stick-slip dynamics of a two degree of freedom system.*Int. Journal of Bifurcation and Chaos* 2003;**13(4)**: 843-861.
10. Awrejcewicz J, Sendkowski D . Stick-slip detection in coupled oscillators with friction.*Int. Journal of Solids and Structures* 2005;**42(21-22)**: 56695682.
11. Stefanski A, Kapitaniak T. Using chaos synchronization to estimate the largest Lyapunov exponent of non-smooth systems.*Discrete Dynamics in Nature and Society* 2000;**4(3)**: 207-215.